

## INTESTINAL INFECTION

# Effect of chronic *Giardia lamblia* infection on epithelial transport and barrier function in human duodenum

Hanno Troeger, Hans-Joerg Epple, Thomas Schneider, Ulrich Wahnschaffe, Reiner Ullrich, Gerd-Dieter Burchard, Tomas Jelinek, Martin Zeitz, Michael Fromm, Joerg-Dieter Schulzke

*Gut* 2007;56:328–335. doi: 10.1136/gut.2006.100198

See end of article for authors' affiliations

Correspondence to: Professor Dr J-D Schulzke, Campus Benjamin Franklin, Charité, Medizinische Klinik I, Gastroenterology, Infectious Diseases and Rheumatology, 12200 Berlin, Germany; joerg.schulzke@charite.de

Revised 24 July 2006  
Accepted 2 August 2006  
Published Online First  
25 August 2006

**Background:** *Giardia lamblia* causes infection of the small intestine, which leads to malabsorption and chronic diarrhoea.

**Aim:** To characterise the inherent pathomechanisms of *G lamblia* infection.

**Methods:** Duodenal biopsy specimens from 13 patients with chronic giardiasis and from controls were obtained endoscopically. Short-circuit current ( $I_{SC}$ ) and mannitol fluxes were measured in miniaturised Ussing chambers. Epithelial and subepithelial resistances were determined by impedance spectroscopy. Mucosal morphometry was performed and tight junction proteins were characterised by immunoblotting. Apoptotic ratio was determined by terminal deoxynucleotidyl transferase-mediated deoxyuridine triphosphate nick-end labelling staining.

**Results:** In giardiasis, mucosal surface area per unit serosa area was decreased to 75% (3%) of control, as a result of which epithelial resistance should increase. Instead, epithelial resistance of giardiasis biopsy specimens was decreased (19 (2) vs 25 (2)  $\Omega$   $cm^2$ ;  $p < 0.05$ ) whereas mannitol flux was not significantly altered (140 (27) vs 105 (16)  $nmol/h/cm^2$ ). As structural correlate, reduced claudin 1 expression and increased epithelial apoptosis were detected. Furthermore, basal  $I_{SC}$  increased from 191 (20) in control to 261 (12)  $\mu A/h/cm^2$  in giardiasis. The bumetanide-sensitive portion of  $I_{SC}$  in giardiasis was also increased (51 (5) vs 20 (9)  $\mu A/h/cm^2$  in control;  $p < 0.05$ ). Finally, phlorizin-sensitive  $Na^+$ -glucose symport was reduced in patients with giardiasis (121 (9) vs 83 (14)  $\mu A/h/cm^2$ ).

**Conclusions:** *G lamblia* infection causes epithelial barrier dysfunction owing to down regulation of the tight junction protein claudin 1 and increased epithelial apoptoses.  $Na^+$ -dependent D-glucose absorption is impaired and active electrogenic anion secretion is activated. Thus, the mechanisms of diarrhoea in human chronic giardiasis comprise leak flux, malabsorptive and secretory components.

The flagellated protozoan *Giardia lamblia* (syn *G duodenalis* and *G intestinalis*) is the most common human gastrointestinal parasite in Western Europe and the US.<sup>1</sup> Furthermore, giardiasis accounts for a considerable proportion of diarrhoeal illnesses worldwide and is frequently encountered in travellers with persistent diarrhoeal complaints.<sup>2</sup>

The disease is characterised by diarrhoea, malaise, steatorrhoea and malabsorption and becomes chronic in approximately 15% of infected individuals.<sup>3,4</sup> A still unexplained feature is the varying severity of clinical disease, with about half of the individuals exposed to *G lamblia* being asymptomatic, which has been observed even after experimental infection with isolates derived from highly symptomatic patients.<sup>5</sup>

*G lamblia* is a non-invasive microorganism, and the major structural and functional abnormalities associated with this disease are found in the small intestine. Human infection can lead to a spectrum of microscopic changes that range from mild abnormalities to subtotal villous atrophy in severe cases. Even in the absence of changes in villous and crypt architecture, the shortening and disruption of microvilli has been reported and is associated with brush border enzyme deficiency, especially lactase deficiency.<sup>6,7</sup> A large study of conventional histological sections showed no pathological findings in 96% of subjects with giardiasis.<sup>8</sup>

The mechanisms of diarrhoea in human chronic giardiasis have not been studied. Insight into potential mechanisms has been gained exclusively from animal models and in vitro studies on a duodenal cell line. However, pathophysiological changes obtained from these models may be difficult to

extrapolate owing to the chronicity of infection and species differences.

Although the first in vitro study did not show an effect of *G lamblia* on human cultured epithelial cells,<sup>9</sup> more recent studies showed a 50% reduction in transepithelial resistance 24 h after *G lamblia* infection, which was associated with increased macromolecule permeability.<sup>10,11</sup> Scott *et al*<sup>12</sup> showed that the *G lamblia*-induced reorganisation of the tight junctional protein ZO-1 and of F-actin is myosin light chain kinase dependent. Recently, the same group showed that an increase in enterocyte apoptosis is a main structural correlate for barrier dysfunction observed after *G lamblia* infection in vitro.<sup>13</sup>

In addition, studies have been performed on rodent infection models.<sup>14–16</sup> Besides the constant finding of villous height reduction,  $Na^+/D$ -glucose malabsorption was a prominent feature. Two of these studies also found an activated chloride secretion.<sup>15,16</sup> More recently, in vivo animal studies confirmed the findings from cell culture models and found an increased intestinal permeability after *G muris* infection, suggesting epithelial barrier dysfunction as another pathomechanism of diarrhoea.<sup>12</sup>

Whether such changes are also responsible for the diarrhoea observed in humans has not yet been investigated. Therefore, this study aimed to examine the effects of *G lamblia* infection on the small intestine of humans by examining duodenal forceps biopsy specimens.

**Abbreviations:** IEL, intraepithelial lymphocytes; TUNEL, terminal deoxynucleotidyl transferase-mediated deoxyuridine triphosphate nick-end labelling;  $I_{SC}$ , short-circuit current

## PATIENTS AND METHODS

### Study subjects

Thirteen symptomatic patients with chronic *G lamblia* infection diagnosed at the Institute of Tropical Medicine, Berlin, Germany, who underwent upper gastrointestinal endoscopy at the University Hospital Campus Benjamin Franklin, Berlin, Germany, were included in the study over a 3-year period between 2002 and 2005. A group of 12 patients who underwent endoscopy in this period of time without macroscopic or microscopic signs of pathology served as controls. All patients gave their written consent to undergo biopsies for scientific purposes and the study was approved by the local ethics committee. The median age was 34 (range 22–64) years in giardiasis and 47 (range 28–70) years in controls.

### Solutions and drugs

The bathing solution of flux experiments contained (in mmol/l)  $\text{Na}^+$  140,  $\text{Cl}^-$  123.8,  $\text{K}^+$  5.4,  $\text{Ca}^{2+}$  1.2,  $\text{Mg}^{2+}$  1.2,  $\text{HPO}_4^{2-}$  2.4,  $\text{H}_2\text{PO}_4^-$  0.6,  $\text{HCO}_3^-$  21,  $\text{D}(+)\text{-glucose}$  10,  $\beta\text{-OH-butyrate}$  0.5, glutamine 2.5,  $\text{D}(+)\text{-mannose}$  10 and mannitol 10. The solution was gassed with 95%  $\text{O}_2$  and 5%  $\text{CO}_2$ . The temperature was maintained at 37°C and pH was 7.4 in all experiments. Antibiotics (50 mg/l piperacillin and 4 mg/l imipenem) served to prevent bacterial growth and had no effect on short-circuit current ( $I_{\text{SC}}$ ) in the concentrations used. Theophylline, prostaglandin  $\text{E}_2$  and phlorizin were purchased from Sigma Chemical (St Louis, Missouri, USA).

### Biopsy protocol

A miniaturised Ussing chamber with an exposed area of 0.049  $\text{cm}^2$  was used as described previously.<sup>17</sup> Measurements were performed on duodenal specimens, which were obtained from the distal duodenum during upper endoscopy by a biopsy forceps with a diameter of 3.4 mm. Biopsy specimens were fixed on a disc with histoacryl tissue glue. The time between taking the biopsy and mounting it into the Ussing chamber was about 20–30 min, during which the specimen was kept on ice in oxygenated phosphate-buffered saline. After an equilibration period of 20 min, impedance spectroscopy, flux measurements and transport studies were performed.

### Impedance spectroscopy

Impedance analysis was performed as described previously.<sup>17–19</sup> This technique can differentiate the epithelial and subepithelial portion of transmural resistance. In this model, the epithelium is described as an electrical equivalent circuit of a resistor and a capacitor in parallel and the subepithelium is described as a resistor in series. After application of 48 discrete frequencies of an effective sine-wave alternating current of 35  $\mu\text{A}/\text{cm}^2$ , ranging from 1.3 Hz to 65 kHz, changes in tissue voltage were detected by phase-sensitive amplifiers (1250 frequency response analyser and 1286 electrochemical interface; Solartron Schlumberger, Farnborough, Hampshire, UK). Complex impedance values were calculated and corrected for the resistance of the bathing solution and the frequency behaviour of the measuring device. Then, for each tissue, the impedance locus was plotted in a Nyquist diagram fitted by least squares analysis. Owing to the frequency-dependent electrical characteristics of the capacitor, transmural wall resistance ( $R^{\text{t}}$ ) is obtained at low frequencies and subepithelial resistance ( $R^{\text{sub}}$ ) is obtained at high frequencies. Epithelial resistance ( $R^{\text{e}}$ ) was obtained from  $R^{\text{e}} = R^{\text{t}} - R^{\text{sub}}$ .

### $I_{\text{SC}}$ and mannitol flux measurements

Ussing-type experiments were performed as described previously using a computer-controlled voltage clamp device (CVC 6; Fiebig, Berlin, Germany).<sup>17, 20</sup> Paracellular permeability was

determined by  $^3\text{H}$ -mannitol flux (mucosal-to-serosal) under short circuit conditions. Briefly,  $10^7$  cpm-labelled mannitol ( $10^{-9}$  mmol/l; specific activity: 20 Ci/mmol; ARC, Missouri, USA) was added to the mucosal side. After an equilibration period, a fraction of the serosal volume was sampled in three 15 min intervals and analysed using a liquid scintillation analyser (Tri-Carb 2100TR; Packard, USA). Basal short circuit current ( $I_{\text{SC}}$ ) was calculated as the mean value of the period of time between minutes 30 and 75. Active electrogenic anion secretion was maximally induced using prostaglandin  $\text{E}_2$  ( $10^{-6}$  mmol/l) on the serosal side and theophylline ( $10^{-2}$  mmol/l) on both sides to test epithelial transport function. As a result, maximum  $I_{\text{SC}}$  values after pharmacological stimulation did not differ significantly between both groups (323 (26)  $\mu\text{mol}/\text{h}/\text{cm}^2$  in control vs 312 (22)  $\mu\text{mol}/\text{h}/\text{cm}^2$  in giardiasis). For quantification of spontaneous active transport rates in both groups, sodium-dependent  $\text{D}$ -glucose transport was detected as  $I_{\text{SC}}$  inhibited by phlorizin ( $5 \times 10^{-4}$  mmol/l at the mucosal side) and active electrogenic chloride secretion as  $I_{\text{SC}}$  inhibited by bumetanide ( $10^{-5}$  mmol/l at the serosal side).

### Histology and apoptosis detection

After the electrophysiological measurements in the Ussing chamber, biopsy specimens were cut off the insert of the chamber, fixed in 10% buffered formalin and embedded in paraffin wax. Serial sections (3  $\mu\text{m}$ ) were stained with H&E, or dewaxed for fluorescence detection of epithelial apoptosis. Cellular DNA was stained with terminal deoxynucleotidyl transferase-mediated deoxyuridine triphosphate nick-end labelling (TUNEL) assay (Roche, Mannheim, Germany). Epithelial apoptosis was determined as the percentage of apoptotic cells per total enterocytes (apoptotic ratio).

### Mucosal morphometry

Morphometry of the mucosal surface area was performed on duodenal tissue still fixed in the Ussing chamber to guarantee the same degree of stretch as in the electrophysiological experiments. Conventional histology and a microdissection procedure were used as described previously.<sup>21</sup> Crypt length and inner crypt diameter were measured in H&E-stained sections. For counting the number of crypts and villi per serosal area, light microscopy was performed using a digital camera. Morphometric analysis of the villous surface area was carried out after microdissection according to Clarke.<sup>21</sup> Distal duodenal biopsy specimens were fixed in ethanol/glacial acetic acid (3:1) for 24 h, and then transferred to and stored in 75% ethanol. After staining with the Feulgen reaction, villi were dissected under a stereomicroscope. The median height of 10 villi was determined. In addition, basal and upper villous diameters were measured to calculate villous surface area. Total mucosal surface area was calculated using this crypt and villous surface area calculation after multiplication with the number of crypts and villi. Data are presented as mucosal surface area per serosal area.

### Western blot analysis of tight junction proteins

To determine tight junction protein expression, Western blot analysis of eight patients was performed on membrane extracts of duodenal biopsy specimens as described previously.<sup>22</sup> Therefore, only those patients in whom lamblia trophozoites had been found in histological sections or duodenal fluid were included. Biopsy specimens were homogenised in iced lysate buffer and then passed through a 26 G  $\times$  1/2-inch needle. The extract was centrifuged at 200  $g$  for 5 min at 4°C. The supernatant was then centrifuged at 43 000  $g$  for 30 min at 4°C. The pellet representing a crude membrane fraction was resuspended in lysate buffer. Protein concentrations were

determined by Pierce BCA assay (Pierce, Rockford, Illinois, USA). Aliquots of 5  $\mu\text{g}$  protein were separated by PAGE (8.5% for occludin and 12.5% for claudins) and transferred to a polyscreen polyvinylidene difluoride transfer membrane (NEN Life Science Products, Boston, Massachusetts, USA). Blots were blocked in milk powder and bovine serum albumin before incubation with primary rabbit polyclonal IgG against claudins 1, 2, 7, occludin and primary monoclonal antibody against claudin 4. Peroxidase-conjugated goat anti-rabbit/anti-mouse IgG and the chemiluminescence detection system Lumi-LightPLUS Western Blotting Kit (Roche, Mannheim, Germany) were used to detect bound antibodies. Antibodies were purchased from Zymed Laboratories (South San Francisco, California, USA). Chemiluminescence signals were detected using an LAS-1000 imaging system (Fuji, Tokyo, Japan) and analysed with the AIDA program package (Raytest, Berlin, Germany).

### Statistical analysis

Results are given as means (SEM). Significance was tested by the two-tailed Student's *t* test.  $p < 0.05$  was considered significant.

## RESULTS

### Mucosal morphometry and histology

Mucosal architecture was altered in the duodenum of patients with chronic giardiasis (fig 1). A detailed morphometrical analysis showed a reduction in villous surface area by 50% with no noticeable changes in crypt morphology. These changes led to an overall reduction of mucosal surface area to 75 (3)% of control tissue (table 1). The number of CD3-positive intra-epithelial lymphocytes (IEL) was increased in giardiasis (44 (6) vs 16 (4) IEL/100 enterocytes;  $p < 0.01$ ).

### Impedance spectroscopy and mannitol flux

Figure 2 shows representative impedance locus plots obtained on duodenal specimens from patients with giardiasis and controls. Table 2 presents the statistical analysis of these data. Compared with controls, a decrease in  $R^c$  was observed in giardiasis. However,  $R^{\text{sub}}$  remained unchanged, resulting in non-significant changes in  $R^t$  between both groups (table 2). Also, in line with the results of the electrophysiological measurements, there was a tendency towards higher mannitol fluxes in giardiasis, which did not reach statistical significance. This parameter, like the ionic permeability determined by measuring the total  $R^t$ , reflects the paracellular pathway. Although these parameters often change in parallel in the small intestine, mannitol permeability can also differ from cation permeability—for example in case of claudin 2

transfection into MDCK cells.<sup>23</sup> Here, only cation permeability of the tight junction was modulated, whereas mannitol flux was not affected. However, in this study on chronic giardiasis, mannitol flux and  $R^t$  showed identical behaviour—namely, a tendency towards an increased permeability without reaching statistical significance (table 2).

### Correction of barrier parameters for surface area changes

Taking the diminished mucosal surface area in giardiasis into account,  $R^c$  as determined by impedance spectroscopy needs to be corrected. For example, without any change in epithelial barrier properties this decrease in mucosal surface area in giardiasis would have led to an apparent increase in  $R^c$ . Thus,  $R^c$  values without surface area correction would overestimate epithelial barrier function in giardiasis. Figure 3 presents the respective corrected values for  $R^c$  and shows that epithelial barrier dysfunction in giardiasis was even more pronounced than assumed from the raw data before correction.

### Transport studies

Another important aspect from impedance spectroscopy is the correction of active transport rates for  $R^{\text{sub}}$  contributions. Whenever significant non-epithelial series resistances are present in addition to the  $R^c$  between the voltage-sensing electrodes, measured  $I_{\text{sc}}$  values have to be corrected for the contribution of additional resistances. This correction is well known for bath resistance, but it is also necessary to correct  $I_{\text{sc}}$  for the contribution of  $R^{\text{sub}}$  of intestinal preparations. The implications of this correction have been given elsewhere in detail.<sup>18 20 24 25</sup> Generally, after correction for the bathing solution, the true active transport rate is underestimated by a factor given by the ratio of  $R^t$  over  $R^c$ . This factor was 2.9 (0.2) in patients with giardiasis and 2.4 (0.1) in controls (table 1). As these factors differed considerably by about 20%,  $I_{\text{sc}}$  values of both groups were compared only after correction (table 3 gives the raw and corrected data for active transport).

Basal  $I_{\text{sc}}$  was increased in giardiasis when compared with controls (table 3). In addition, inhibition of  $I_{\text{sc}}$  by bumetanide, an inhibitor of the sodium-2 chloride-potassium-cotransporter and thereby an inhibitor of rheogenic chloride secretion, was higher in giardiasis than in controls (table 3). The reason why this inhibition reached only 20% of  $I_{\text{sc}}$  in both groups is due to the fact that in bicarbonate-containing bathing solutions other anion transport mechanisms contribute to the overall rheogenic ion transport. Taken together, these data indicate that active anion secretion is activated in both mucosae, but to a higher degree in patients with giardiasis than in controls.

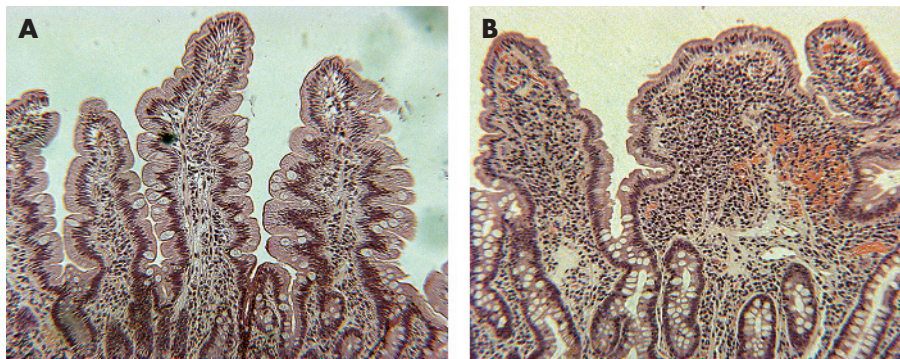


**Figure 1** Thin sections of biopsy specimens from the duodenum of a control (A) and a patient with chronic giardiasis (B) stained with H&E (original magnification 20 $\times$ ).



**Table 1** Morphometric analysis of duodenal mucosa

	Control	Giardiasis	p Value
Villus height ( $\mu\text{m}$ )	445 (23)	314 (11)	<0.001
Villus breadth at apex ( $\mu\text{m}$ )	181 (11)	132 (6)	<0.001
Villus breadth at base ( $\mu\text{m}$ )	212 (11)	171 (9)	<0.01
Villi per serosal area ( $\text{mm}^{-2}$ )	11 (0.3)	11 (0.5)	NS
Villous surface ( $\text{mm}^2$ )	0.22 (0.02)	0.11 (0.01)	<0.001
Crypt length ( $\mu\text{m}$ )	219 (6)	230 (10)	NS
Inner crypt diameter ( $\mu\text{m}$ )	12 (0.5)	13 (0.9)	NS
Crypts per serosal area ( $\text{mm}^{-2}$ )	157 (9)	138 (6)	NS
Mucosal surface per area ( $\text{mm}^2/\text{mm}^2$ )	5.1 (0.3)	3.9 (0.2)	<0.001

NS, not significant.

Mucosal surface area morphometry of duodenal specimens obtained from microdissection and conventional histology as described under the Patients and methods section. Data represent means (SEM).

As another important active epithelial transport system Na-glucose symport was studied. For this purpose, phlorizin was used as an inhibitor of the sodium-glucose-cotransporter 1. The respective decrease in  $I_{\text{sc}}$  was used to quantify Na-dependent D-glucose absorption. The phlorizin-dependent reduction in  $I_{\text{sc}}$  was less pronounced in giardiasis than in controls, pointing to an impaired transport function (table 3).

### Epithelial apoptosis

Typical apoptotic changes associated with epithelial apoptosis comprise condensation of chromatin, its compaction along the periphery of the nucleus and segmentation of the nucleus in conjunction with a positive staining with TUNEL (fig 4, arrows). In controls, apoptotic ratio amounted to 1 (0.1)% of the total enterocyte count, whereas in giardiasis epithelial apoptotic ratio was moderately increased to 1.5 (0.2)% ( $p < 0.05$ , fig 4).

### Tight junction protein expression

To further investigate epithelial barrier dysfunction in giardiasis, tight junction protein expression was studied by immunoblot analyses of the tight junctional proteins claudin 1, 2, 4, 7 and occludin. As these proteins are integral membrane proteins forming tight junction strands, membrane fractions were used for the analysis. Figure 5 gives the respective data. Densitometry of western blots showed a decreased expression of claudin 1, 4 and 7 in the analysis of the raw data. After subsequent correction for the reduction of mucosal surface area in giardiasis, only claudin 1 expression differed significantly from controls (decreased to 71% of control level). Claudin 2 was not detectable either in controls or in patients with giardiasis, even if the protein load was increased to 20  $\mu\text{g}$  per lane.

### DISCUSSION

This study aimed to characterise the pathomechanisms of diarrhoea and malabsorption in human small intestines chronically infected with *G lamblia*. In general, diarrhoea can be driven by changes in motility or by osmotic forces, and osmotic forces can result from active secretion, leak flux mechanisms and malabsorption.

As the first important finding of our study, impedance spectroscopy showed  $R^e$  that was considerably reduced in chronic giardiasis. However,  $R^{\text{sub}}$ , and hence  $R^t$ , was not altered considerably. This underlines the importance of applying impedance spectroscopy for investigating diseased mucosae, as conventional resistance analysis would have missed this epithelial barrier dysfunction. At first glance, the degree of this barrier disturbance seemed to be rather low. However, one has to keep in mind that mucosal surface area is markedly reduced. Taking this into account, epithelial barrier dysfunction has to be assumed to be significant. The first evidence for an epithelial change with increased intestinal permeability in giardiasis came from infants, using the lactulose-mannitol ratio, as well as from adults, using technetium-labelled DTPA.<sup>26, 27</sup> Furthermore, mice infected with *G muris* showed increased intestinal permeability from day 4 until day 21 after infection.<sup>12</sup> However, these techniques cannot exclude area or blood flow changes as possible confounding factors. More direct evidence for epithelial barrier impairment in giardiasis resulted from in vitro studies. Here, the addition of *G lamblia* sonicates on to the duodenal cell line SCBN showed decreased resistance and increased FITC-dextran 3000 fluxes.<sup>11</sup> After barrier dysfunction had been shown by rather indirect methods in human and animal models and by direct methods in the in vitro studies, our data from human biopsy specimens are the first that directly quantify this barrier dysfunction in human chronic giardiasis.

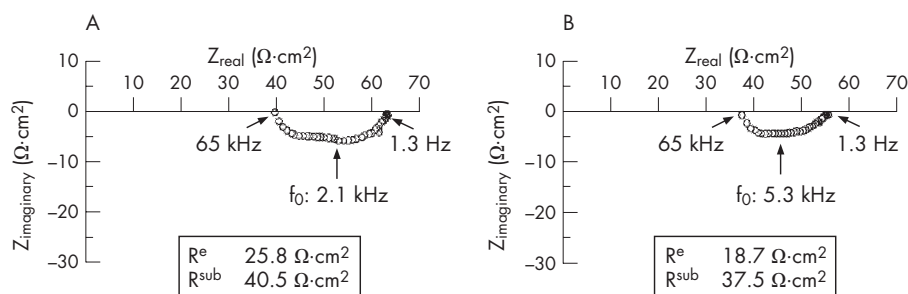


**Figure 2** Original impedance locus plots of the human duodenum: (A) control and (B) giardiasis.  $Z_{\text{real}}$  gives the ohmic component and  $Z_{\text{imaginary}}$  the reactive component of the complex impedance. Intersections between the semicircle and x axis at low and high frequencies represent  $R^t$  and  $R^{\text{sub}}$ , respectively.  $R^t$  minus  $R^{\text{sub}}$  equals  $R^e$ . For a detailed explanation of transepithelial impedance data, see Gitter *et al.*<sup>13</sup>

**Table 2** Electrical resistance and mannitol flux

	R <sup>t</sup> (Ω cm <sup>2</sup> )	R <sup>e</sup> (Ω cm <sup>2</sup> )	R <sup>sub</sup> (Ω cm <sup>2</sup> )	R <sup>t</sup> /R <sup>e</sup>	J <sub>Man</sub> (nmol/h/cm <sup>2</sup> )	n
Control	59 (4)	25 (2)	34 (2)	2.4 (0.1)	105 (16)	12
Giardiasis	52 (3)	19 (2)	33 (2)	2.9 (0.2)	140 (27)	12
p Value	NS	<0.05	NS	<0.05	NS	

NS, not significant.

Transmural wall resistance (R<sup>t</sup>) as well as epithelial (R<sup>e</sup>) and subepithelial (R<sup>sub</sup>) resistance portions as determined by impedance spectroscopy. R<sup>t</sup>/R<sup>e</sup> is the correction factor of active transport rates (eg, I<sub>sc</sub> values) for R<sup>sub</sup> contributions as described under the Results section. Mannitol flux (J<sub>Man</sub>) was measured as unidirectional flux in m-to-s direction in the Ussing chamber. All data represent means (SEM).

This *G lamblia*-induced epithelial barrier dysfunction contributes to diarrhoea by a leak flux mechanism. Normally, the epithelial barrier maintains the “milieu intérieur”. If it is defective, solutes and water will enter the lumen depending on the permeability of the paracellular pathway. Evidence that a leak flux mechanism is sufficient to elicit diarrhoea was already obtained in HIV enteropathy, where barrier dysfunction was primarily responsible for relevant diarrhoea in these patients.<sup>17</sup> This form of diarrhoea was also found to be induced by *Clostridium difficile*.<sup>28</sup> More direct evidence for this concept comes from Fasano *et al.*<sup>29</sup> Attenuated *Vibrio cholerae* strains depleted of the chloride secretion-inducing cholera toxin gene were shown to still induce diarrhoea in human volunteers. This results from another toxin, zonula occludens toxin, which leads to a change in tight junction structure, and consequently ions and water are lost into the intestinal lumen.

When further investigating the nature of epithelial barrier dysfunction in patients with chronic lambliasis, we found that the epithelial apoptotic rate was increased by >50%. This is in accordance with previous in vitro studies showing that apoptotic events are stimulated in enterocytes after *G lamblia* infection and that this is a caspase-3-dependent process.<sup>13</sup> However, the total increase in apoptotic ratio was only moderate (a 0.5% increase) compared with the in vitro observations mentioned above or to other small intestinal diseases such as HIV enteropathy where the apoptotic ratio reaches a level as high as 4%.<sup>30</sup> Nevertheless, it is well established that epithelial apoptoses can play an important role for epithelial barrier function, even if the increase is only moderate.<sup>22 31 32</sup> Although it was originally thought that

epithelial apoptosis at the villus tip is a regular and highly sealed process without much barrier importance, our own group has presented experimental data that apoptoses possess marked conductivity.<sup>33</sup> In addition, apoptotic foci were directly demonstrated to contribute to the barrier dysfunction in ulcerative colitis using the conductance scanning technique.<sup>34</sup> Thus, the relative contribution of apoptotic events may vary from minor to predominating, depending on the particular condition. The relatively weak increase in apoptotic rates in patients with giardiasis represents a relevant contribution to epithelial pathology but seems to play a rather moderate role for barrier dysfunction and diarrhoea. Presumably, apoptosis is triggered by direct contact of the parasites or their products with the epithelium as shown in in vitro studies using monolayers of duodenum-derived cells.<sup>13</sup> On the other hand, even if *G lamblia* does not cause heavy local inflammation in the intestine, it is feasible that even low-level release of pro-inflammatory cytokines such as tumour necrosis factor α or interferon-γ could lead to increased epithelial apoptosis in response to the chronic colonisation.

Besides epithelial apoptosis, tight junctions are one of the prominent features that determine epithelial barrier properties.<sup>35</sup> The epithelial tight junction forms a barrier between neighbouring epithelial cells, which limits transepithelial movement of ions and solutes through the paracellular route. Thus, tight junctions are also a target of pathophysiological stimuli through pathogens.<sup>36 37</sup> On first view, nearly all the examined tight junctional proteins seemed to be decreased in chronic giardiasis. However, this was mainly caused by the serious reduction in mucosal surface area, which in itself causes a reduction in the epithelial tight junction protein pool. Therefore, after mucosal surface correction, only claudin 1 expression was differentially downregulated in chronic giardiasis. Claudin 1 is known to have sealing properties as, for example, indicated by an increase in barrier function after overexpression in epithelial monolayers.<sup>38</sup> Furthermore, claudin

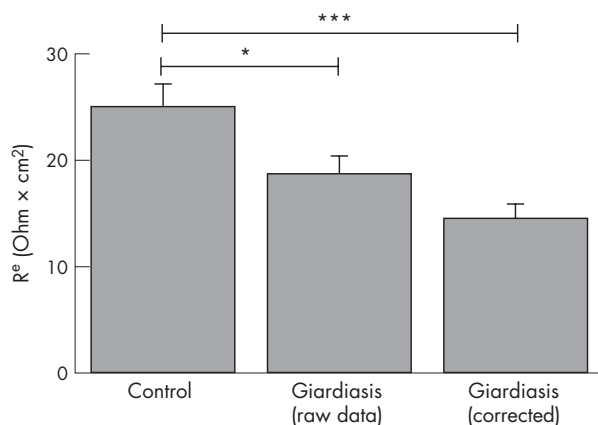


**Figure 3** Epithelial resistance of duodenal specimens obtained from patients with chronic giardiasis and controls as determined by impedance spectroscopy. In addition, epithelial resistance was shown after correction for the reduction of mucosal surface area in giardiasis as described under the Methods section. Data are means (SEM). \*p<0.05; \*\*\*p<0.001.

**Table 3** Active epithelial transport in giardiasis

	I <sub>sc</sub> basal (μmol/h/cm <sup>2</sup> )	ΔI <sub>sc</sub> bumetanide (μmol/h/cm <sup>2</sup> )	ΔI <sub>sc</sub> phlorizin (μmol/h/cm <sup>2</sup> )	n
Raw data				
Control	79 (7)	8 (4)	51 (3)	12
Giardiasis	98 (8)	18 (2)	32 (7)	12
Corrected data				
Control	191 (20)	20 (9)	121 (9)	12
Giardiasis	261 (12)	51 (5)	83 (14)	12
p Value	<0.01	<0.05	<0.05	

Short-circuit current (I<sub>sc</sub>) under basal conditions (I<sub>sc</sub> basal) and change in I<sub>sc</sub> after the addition of phlorizin (ΔI<sub>sc</sub> phlorizin) and bumetanide (ΔI<sub>sc</sub> bumetanide), respectively. Data are presented before (raw data) and after correction for the epithelial–subepithelial resistance ratio. All data represent means (SEM).

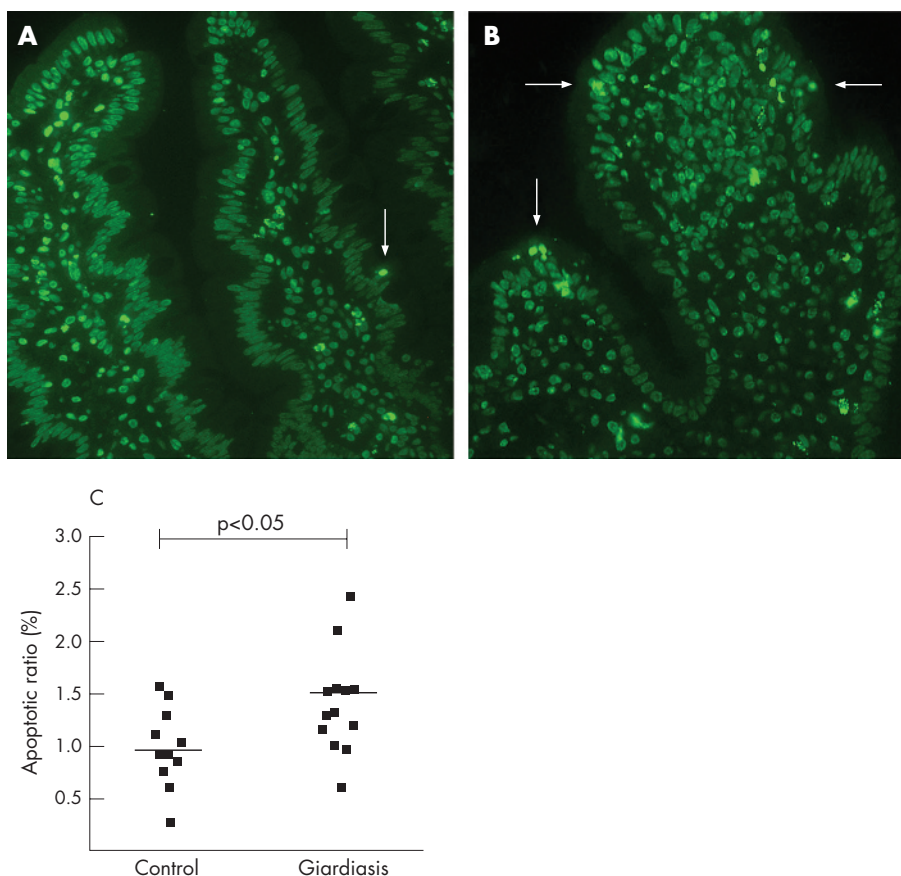


**Figure 4** Epithelial apoptoses indicated by terminal deoxynucleotidyl transferase-mediated deoxyuridine triphosphate nick-end labelling staining in thin sections of duodenal specimens (original magnification 20×). (A) Control and (B) patient with giardiasis. Condensed chromatin fragments in nuclei and segmentation of the nuclei indicate epithelial apoptoses (arrows). (C) Apoptotic ratios of controls (n = 11) and patients with giardiasis (n = 13), which are presented individually as well as mean values (black lines).

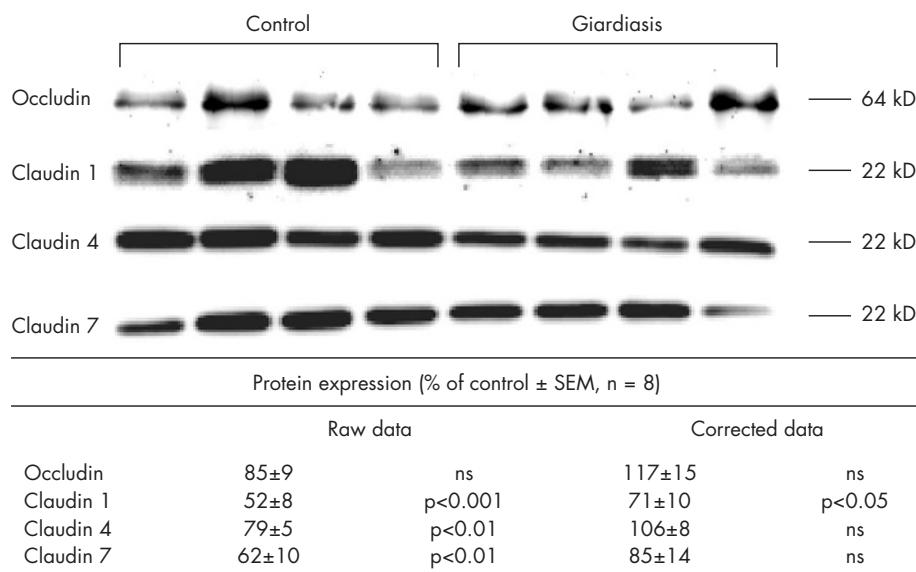


**Figure 5** Tight junction proteins occludin and claudin 1, 4 and 7. Expression was analysed in membrane fractions by immunoblotting and subsequent densitometry. Each lane represents one biopsy. Lanes 1–4 represent samples from the duodenum of controls, and lanes 5–8 represent samples from patients with giardiasis. A second immunoblot was run on four further patients and four further controls (data not shown). The statistical evaluation of densitometric data represents protein expression of the eight patients with giardiasis (in percentage of all controls on the same blot). Raw data were subsequently corrected for mucosal surface area changes. All data are given as means (SEM).

1 knock-out mice were shown to die shortly after birth owing to a loss of water through the leaky epidermis.<sup>39</sup> Therefore, the decreased expression of claudin 1 has to be assumed to be another relevant structural correlate for the decreased epithelial resistance in chronic human giardiasis. Claudin 2, a protein with pore-forming properties, which is primarily expressed in the crypt regions,<sup>23, 40</sup> was not detectable. This may reflect the rather low level of mucosal inflammation in giardiasis,<sup>41</sup> as up regulation of claudin 2 had been shown under inflammatory conditions in ulcerative colitis and duodenal HIV enteropathy using the same technique.<sup>42, 30</sup>

As another important observation, an increase in basal  $I_{sc}$  was found in chronic giardiasis. Such an increase in spontaneous  $I_{sc}$  in the presence of phlorizin usually reflects increased active anion (chloride/bicarbonate) secretion. This was supported by the blocking effect of bumetanide, which was considerably higher in giardiasis than in controls. In keeping with these findings in human biopsy specimens, previous reports have also shown chloride secretion to be activated in the small intestine of mice infected with *G lamblia*.<sup>15, 16</sup> Noteworthy, this anion secretion is activated in giardiasis despite the reduction in mucosal surface area. However, mucosal surface reduction in our study is predominantly due to villous surface reduction, whereas crypts as an important source of active anion secretion<sup>43</sup> were not affected. Interestingly, active anion secretion was also observed in HIV enteropathy, and this was thought to result from an altered cytokine pattern released from the HIV-infected subepithelial immune cells.<sup>44</sup> Therefore, it may be reasonable to assume that the activation of active anion secretion in giardiasis could also be induced by an altered cytokine pattern.

Finally, we observed an impaired sodium-coupled D-glucose absorption in the duodenum of patients chronically infected with *G lamblia*. This was not surprising, as the mucosal surface area was considerably affected. Thus, the crucial factor for this glucose malabsorption seems to be the reduction in villous surface area, as the degree of the Na-glucose symport reduction did not substantially exceed the degree of mucosal surface decrease. However, it should be noted that overall loss of absorptive surface area may occur even in the absence of villous atrophy—namely, via a diffuse shortening of brush border microvilli, a mechanism that has been previously described in giardiasis.<sup>6, 14</sup> Furthermore, it was shown in a mouse model that IEL can induce brush border injury and malfunction.<sup>45</sup> Interestingly, we observed an increased number of IEL in giardiasis, which may cause brush border changes and would be a further explanation for the Na-glucose malabsorption observed in our study.

A variable degree of mucosal architecture change is established in giardiasis in humans as well as from data obtained in animal models. This is generally assumed to account for the malabsorptive component of the diarrhoea in giardiasis.<sup>14, 16</sup> On the other hand, it is in sharp contrast with a large histological analysis that detected a change in villous architecture only in a minority of patients.<sup>8</sup> In our own study, we were surprised to find a reduction in villous surface area in almost all specimens from individuals with chronic giardiasis. This may reflect the selected group of patients with pronounced chronic complaints, which were referred to our university centre for more extensive diagnostic procedures including upper gastrointestinal endoscopy. Furthermore and more important, it could also be due to the microdissection technique used in present protocol, which is a very sensitive method to analyse villous surface area changes. This is also supported by the fact that routine histological analysis of our specimens in the pathology department showed an altered mucosal architecture in only two thirds of the specimens (data not shown).

In conclusion, chronic infection of *G lamblia* in humans leads to a combination of epithelial transport and barrier dysfunction. We showed a dramatic reduction in villous surface, which in turn leads to reduced absorptive capacity as shown by reduced Na-glucose absorption. Moreover, duodenal mucosa exhibited increased anion secretion. Hence, malabsorption and active secretion as shown in animal models also seem extremely important in human disease. Furthermore, epithelial barrier dysfunction due to chronic *G lamblia* infection could be shown by impedance spectroscopy and, moreover, underlying molecular changes were identified—namely, a reduction in claudin 1 expression and increased epithelial apoptosis.

## ACKNOWLEDGEMENTS

We thank A Fromm, S Schön, U Schreiber and D Sorgenfrei for their outstanding technical assistance, the Endoscopy Unit, Department of Gastroenterology, CBF, Charité, Berlin, for excellent cooperation and Dr Loddenkemper for help with CD3 staining.

## Authors' affiliations

**Hanno Troeger, Hans-Joerg Eppe, Thomas Schneider, Ulrich Wahnschaffe, Reiner Ullrich, Martin Zeitz, Joerg-Dieter Schulzke,** Department of Gastroenterology, Infectious Diseases and Rheumatology, Campus Benjamin Franklin, Charité, Berlin, Germany  
**Michael Fromm,** Institute of Clinical Physiology, Campus Benjamin Franklin, Charité, Berlin, Germany  
**Gerd-Dieter Burchard,** Bernhard-Nocht-Institute for Tropical Medicine, Hamburg, Germany  
**Tomas Jelinek,** Berlin Center For Travel & Tropical Medicine, Berlin, Germany

Funding: This work was supported by grants from the Deutsche Forschungsgemeinschaft (DFG): KFO 104/7 (Clinical Research Unit).

Competing interests: None.

## REFERENCES

- Furness BW, Beach MJ, Roberts JM. Giardiasis surveillance—United States, 1992–1997. *MMWR CDC Surveill Summ* 2000;**49**:1–13.
- Taylor DN, Houston R, Shlim DR. Etiology of diarrhea among travelers and foreign residents in Nepal. *JAMA* 1988;**260**:1245–8.
- Rendtorff RC. The experimental transmission of human intestinal protozoan parasites: II. *Giardia lamblia* cysts given in capsules. *Am J Trop Med Hyg* 1954;**59**:209.
- Adam RD. The biology of *Giardia* spp. *Microbiol Rev* 1991;**55**:706–32.
- Nash TE, Herrington DA, Losonsky GA, et al. Experimental human infections with *Giardia lamblia*. *J Infect Dis* 1987;**156**:974–84.
- Buret A, Gall DG, Olson ME. Growth, activities of enzymes in the small intestine, and ultrastructure of microvillous border in gerbils infected with *Giardia duodenalis*. *Parasitol Res* 1991;**77**:109–14.
- Singh KD, Bhasin DK, Rana SV, et al. Effect of *Giardia lamblia* on duodenal disaccharidase levels in humans. *Trop Gastroenterol* 2000;**21**:174–6.
- Oberhuber G, Kastner N, Stolte M. Giardiasis: a histologic analysis of 567 cases. *Scand J Gastroenterol* 1997;**32**:48–51.
- Chavez B, Knaippe F, Gomez-Mariscal L, et al. *Giardia lamblia*: electrophysiology and ultrastructure of cytopathology in cultured epithelial cells. *Exp Parasitol* 1986;**61**:379–89.
- Teoh DA, Kamieniecki D, Pang G, et al. *Giardia lamblia* rearranges F-actin and  $\alpha$ -actinin in human colonic and duodenal monolayers and reduces transepithelial electrical resistance. *J Parasitol* 2000;**86**:800–6.
- Buret AG, Mitchell K, Muench DG, et al. *Giardia lamblia* disrupts tight junctional ZO-1 and increases permeability in non-transformed human small intestinal epithelial monolayers: effects of epidermal growth factor. *Parasitology* 2002;**125**(Jul):11–19.
- Scott KGE, Meddings JB, Kirk DR, et al. Intestinal infection with *Giardia* spp. reduces epithelial barrier function in a myosin light chain kinase-dependent fashion. *Gastroenterology* 2002;**123**:1179–90.
- Chin AC, Teoh DA, Scott KGE, et al. Strain-dependent induction of enterocyte apoptosis by *Giardia lamblia* disrupts epithelial barrier function in a caspase-3-dependent manner. *Infect Immun* 2002;**70**:3673–80.
- Buret A, Hardin JA, Olson ME, et al. Pathophysiology of small intestinal malabsorption in gerbils infected with *giardia lamblia*. *Gastroenterology* 1992;**103**:506–13.
- Gorowara S, Ganguly NK, Mahajan RC, et al. Study on the mechanism of *Giardia lamblia* induced diarrhoea in mice. *Biochim Biophys Acta* 1992;**1138**:122–6.
- Cevallos A, Carnaby S, James M, et al. Small intestinal injury in a neonatal rat model of giardiasis is strain dependent. *Gastroenterology* 1995;**109**:766–73.



- 17 **Stockmann M**, Fromm M, Schmitz H, *et al.* Duodenal biopsies of HIV-infected patients with diarrhea exhibit epithelial barrier defects but no active secretion. *AIDS* 1998;**12**:43–51.
- 18 **Gitter AH**, Schulzke JD, Sorgenfrei D, *et al.* Ussing-chamber for high-frequency transmural impedance analysis of epithelial tissues. *J Biochem Biophys Methods* 1997;**35**:81–8.
- 19 **Stockmann M**, Gitter AH, Sorgenfrei D, *et al.* Low edge damage container insert that adjusts intestinal forceps biopsies into Ussing-chamber systems. *Pflügers Arch* 1999;**438**:107–12.
- 20 **Schulzke JD**, Fromm M, Bentzel CJ, *et al.* Epithelial ion transport in the experimental short bowel syndrome of the rat. *Gastroenterology* 1992;**102**:497–504.
- 21 **Clarke RM**. Mucosal architecture and epithelial cell production rate in the small intestine of the albino rat. *J Anat* 1970;**107**:519–29.
- 22 **Zeissig S**, Bojarski C, Buerger N, *et al.* Downregulation of epithelial apoptosis and barrier repair in active Crohn's disease by tumour necrosis factor alpha antibody treatment. *Gut* 2004;**53**:1295–302.
- 23 **Amasheh S**, Meiri N, Gitter AH, *et al.* Claudin-2 expression induces cation-selective channels in tight junctions of epithelial cells. *J Cell Sci* 2002;**115**:4969–76.
- 24 **Tai YH**, Tai CY. The conventional short-circuiting technique under-short-circuits most epithelia. *J Membr Biol* 1981;**59**:173–7.
- 25 **Fromm M**, Schulzke JD, Hegel U. Epithelial and subepithelial contributions to transmural electrical resistance of intact rat jejunum in vitro. *Pflügers Arch* 1985;**405**:400–2.
- 26 **Dagci H**, Ustun S, Taner MS, *et al.* Protozoon infections and intestinal permeability. *Acta Trop* 2002;**81**:1–5.
- 27 **Goto R**, Panter-Brick C, Northrop-Clewes CA. Poor intestinal permeability in mildly stunted Nepali children: associations with weaning practices and *Giardia lamblia* infection. *Br J Nutr* 2002;**88**:109–10.
- 28 **Moore R**, Pathoulakis C, LaMont JT, *et al.* *C. difficile* toxin A increases intestinal permeability and induces Cl<sup>-</sup> secretion. *Am J Physiol* 1990;**259**:G165–72.
- 29 **Fasano A**, Baudry B, Pumphlin DW, *et al.* *Vibrio cholerae* produces a second enterotoxin, which affects intestinal tight junctions. *Proc Natl Acad Sci USA* 1991;**88**:5242–6.
- 30 **Epple HJ**, Troeger H, Ullrich R, *et al.* Restitution of HIV-induced intestinal barrier impairment by highly active antiretroviral therapy (HAART). *Gastroenterology* 2005;**128**(Suppl 2):A-541.
- 31 **Bojarski C**, Gitter AH, Bendfeldt K, *et al.* Permeability of human HT-29/B6 colonic epithelium as a function of apoptosis. *J Physiol* 2001;**535**:541–52.
- 32 **Chin AC**, Vergnolle N, MacNaughton WK, *et al.* Proteinase-activated receptor 1 activation induces epithelial apoptosis and increases intestinal permeability. *Proc Natl Acad Sci USA* 2003;**100**:11104–9.
- 33 **Gitter AH**, Bendfeldt K, Schulzke JD, *et al.* Leaks in the epithelial barrier caused by spontaneous and TNF-alpha-induced single-cell apoptosis. *FASEB J* 2000;**14**:1749–53.
- 34 **Gitter AH**, Wullstein F, Fromm M, *et al.* Epithelial barrier defects in ulcerative colitis: characterization and quantification by electrophysiological imaging. *Gastroenterology* 2001;**121**:1320–8.
- 35 **Van Itallie CM**, Anderson JM. The molecular physiology of tight junction pores. *Physiology* 2004;**19**:331–8.
- 36 **Berkes J**, Viswanathan VK, Savkovic SD. Intestinal epithelial responses to enteric pathogens: effects on the tight junction barrier, ion transport, and inflammation. *Gut* 2003;**52**:439–51.
- 37 **Fasano A**, Nataro JP. Intestinal epithelial tight junctions as targets for enteric bacteria-derived toxins. *Adv Drug Deliv Rev* 2004;**56**:795–807.
- 38 **Inai T**, Kobayashi J, Shibata Y. Claudin-1 contributes to the epithelial barrier function in MDCK cells. *Eur J Cell Biol* 1999;**78**:849–55.
- 39 **Furuse M**, Hata M, Furuse K, *et al.* Claudin-based tight junctions are crucial for the mammalian epidermal barrier: a lesson from claudin-1-deficient mice. *J Cell Biol* 2002;**156**:1099–111.
- 40 **Escaffit F**, Boudreau F, Beaulieu JF. Differential expression of claudin-2 along the human intestine: implication of GATA-4 in the maintenance of claudin-2 in differentiating cells. *J Cell Physiol* 2005;**203**:15–26.
- 41 **Eckmann L**. Mucosal defences against *Giardia*. *Parasite Immunology* 2003;**25**:259–70.
- 42 **Heller F**, Florian P, Bojarski C, *et al.* Interleukin-13 is the key effector Th2 cytokine in ulcerative colitis that affects epithelial tight junctions, apoptosis, and cell restitution. *Gastroenterology* 2005;**129**:550–64.
- 43 **Welsh MJ**, Smith PL, Fromm M, *et al.* Crypts are the site of intestinal fluid and electrolyte secretion. *Science* 1982;**218**:1219–21.
- 44 **Schmitz H**, Rokos K, Florian P, *et al.* Supernatants of HIV-infected immune cells affect the barrier function of human HT-29/B6 intestinal epithelial cells. *AIDS* 2002;**16**:983–91.
- 45 **Scott KGE**, Yu LCH, Buret AG. Role of CD8<sup>+</sup> and CD4<sup>+</sup> T lymphocytes in jejunal mucosa injury during murine giardiasis. *Infect Immun* 2004;**72**:3536–42.

## bmjupdates+

bmjupdates+ is a unique and free alerting service, designed to keep you up to date with the medical literature that is truly important to your practice.

bmjupdates+ will alert you to important new research and will provide you with the best new evidence concerning important advances in health care, tailored to your medical interests and time demands.

### Where does the information come from?

bmjupdates+ applies an expert critical appraisal filter to over 100 top medical journals. A panel of over 2000 physicians find the few 'must read' studies for each area of clinical interest.

Sign up to receive your tailored email alerts, searching access and more...

[www.bmjupdates.com](http://www.bmjupdates.com)